Available online at www.sciencedirect.com

Journal of Catalysis 229 (2005) 1–11

JOURNAL OF CATALYSIS

www.elsevier.com/locate/jcat

# Deep oxidation of light alkanes over titania-supported palladium/vanadium catalysts

Tomas Garcia, Benjamin Solsona, Damien M. Murphy, Karen L. Antcliff, Stuart H. Taylor *

*Cardiff University, School of Chemistry, PO Box 912, Cardiff, Cf10 3TB, UK*

Received 5 July 2004; revised 10 September 2004; accepted 17 September 2004

## Abstract

The total oxidation of short-chain hydrocarbons has been studied using a titania-supported palladium catalyst modified with vanadium. A range of catalysts has been prepared by coimpregnation of the titania support with palladium (II) chloride and ammonium metavanadate. The addition of vanadium promoted the rates of oxidation at lower temperatures. Vanadium loadings between 0.5 and 3.0 wt% were investigated and the most active catalyst was 0.5% Pd1.5% V/$TiO_2$. The addition of vanadium decreased the palladium dispersion and the number of surface palladium sites. Microlaser Raman characterisation identified the supported vanadium species and the vanadium loading influenced these. The addition of palladium modified the vanadium species. In particular the presence of palladium increased the concentration of polymeric vanadium species. Temperature-programmed reduction studies showed that the addition of palladium to V/$TiO_2$ significantly increased the ease of catalyst reduction. Characterisation using electron paramagnetic resonance spectroscopy showed that the presence of palladium significantly increased the concentration of $V^{4+}$ species. It is proposed that the increased catalyst activity is related to the modified redox properties of the catalysts.

*Keywords:* Methane; Ethane; Propane; *n*-Butane; Catalytic oxidation; VOCs; Palladium; Vanadium; Titania

## 1. Introduction

In recent years environmental legislation has imposed increasingly stringent targets for permitted levels of atmospheric emission. The emission of volatile organic compounds (VOCs) has received particular attention as they have been established with the increase in photochemical smog [1], depletion of atmospheric ozone [2], and the production of ground-level ozone [3]. VOCs are a wide-ranging class of chemicals, and currently over 300 compounds are classed as VOCs by the US EPA. Although the scale of their discharge is not known it was estimated that at least 20 million tons were released from the US alone in 2000 [4]. US VOC emissions have decreased by about 40% over the past 20 years, but further efforts are still required to limit emissions. Similarly in Europe the Gothenburg Protocol adopted by the 15 EU member states in 1999 requires a 40% reduction in VOC emissions by 2010. In view of the scale of the problem presented to the chemical and processing industries the major challenge they face is to reduce the emission of polluting VOCs with minimal economic impact.

Many different technologies have been developed for VOC abatement, but one of the most versatile is catalytic oxidation to carbon dioxide. Catalytic oxidation offers the advantage that VOCs can be removed from aerial effluents to very low levels. More importantly, in contrast to thermal incineration, the lower temperatures used result in a more economical process and the potential for the production of toxic by-products such as dioxins and $NO_x$ are significantly reduced. Studies of catalytic VOC oxidation have shown that short-chain hydrocarbons are amongs the

---

[*] Corresponding author. Fax: +44 (0)29 2087 4030
*E-mail address:* taylorsh@cardiff.ac.uk (S.H. Taylor).

0021-9517/$ – see front matter © 2004 Elsevier Inc. All rights reserved.
doi:10.1016/j.jcat.2004.09.018

most difficult to destroy [5]. These VOCs are also potent greenhouse gases and the development of more efficient catalysts for their effective abatement is a major research aim.

Generally, noble metal catalysts, such as Pt and Pd dispersed on a high area metal oxide, are the commercial catalysts of choice due to their high intrinsic oxidation activity. It is widely accepted that supported palladium catalysts are the most active for the total oxidation of short-chain alkanes [6]. This high activity has been attributed to the fact that not only metallic palladium but also palladium oxides are active oxidation catalysts. Nevertheless, their catalytic behaviour is not fully understood; for example, the nature of the true active phase, metal or metal oxide, remains a matter of discussion [7]. In the literature many studies have focussed on Pd supported on $\gamma$-$Al_2O_3$ [8–11]. Such catalysts have two major advantages—low manufacturing costs and high specific surface area—but often they are not very stable and show deactivation due to the high temperatures used [12]. Although $\gamma$-$Al_2O_3$ is the most commonly used support, many studies have demonstrated that the catalytic activities of alumina-supported catalysts are lower than those of catalysts supported on other oxides, such as $TiO_2$, $ZrO_2$ and $SnO_2$ [13–17].

The modification of Pd-based catalysts by addition of various promoters, usually metals or metal oxides, has also been investigated. Although in many cases the mechanisms are not well understood, alloying phenomena and modification of the properties of the support are considered as the most important factors. Promoted catalysts usually present higher conversions, better selectivities, and extended resistance to deactivation. It has been shown that the modification of $Pd/Al_2O_3$ catalysts with titania can decrease the bond strength of Pd–O and promotes the reduction/decomposition of PdO to metallic Pd [18]. Other additives have also been used in order to improve the activity and deactivation resistance of Pd-based catalyst supported on alumina. These include $V_2O_5$, $La_2O_3$, $CeO_2$, $ZrO_2$, and BaO [19–24]. It has been reported that promoted $Pd/Al_2O_3$ catalysts present better performance than unmodified $Pd/Al_2O_3$ catalysts for methane deep oxidation [23]. For vanadium-promoted $Pd/Al_2O_3$ catalyst, it has been shown that the increase of catalytic activity could be due to different effects. Neyertz and Volpe [24] reported that the improvement was due to a change produced in the palladium reducibility and the particle size of the binary system, from those corresponding to the unpromoted $Pd/Al_2O_3$. On the other hand, Escandón et al. [19] showed that the increase of the activity could be produced by Pd–V interactions or a modification of the support properties. However, there are no studies on vanadia-modified titania-supported Pd catalysts for the combustion of short-chain alkanes. In this work, we present a study of the activity and characterisation of a range of Pd-supported catalysts on $TiO_2$ modified with vanadia.

## 2. Experimental

### 2.1. Catalyst preparation

The catalysts were prepared by dissolving a known amount of $PdCl_2$ (Aldrich 99%) in 100 ml of deionised water. The solution was heated to 80 °C and stirred continuously. An appropriate quantity of ammonium metavanadate (Aldrich 99+%) and oxalic acid (1.59 g, Aldrich 99+%) was added to the solution of $PdCl_2$. Titanium oxide (19.60 g, Degussa P25. $SA_{BET} = 50\ m^2\ g^{-1}$) was added to the heated solution and stirred at 80 °C to form a paste. The resulting paste was dried at 110 °C for 16 h. The catalyst contained 0.5–2.0 wt% Pd and V in the range 0.5–3.0 wt%. A similar method was used to prepare $TiO_2$-based materials without vanadium and without palladium. Final catalysts were prepared by calcination in static air at 550 °C for 6 h. The range of catalysts prepared is detailed in Table 1.

### 2.2. Catalyst characterisation

Catalyst surface areas were determined by multi point $N_2$ adsorption at 77 K, and data were treated in accordance with the BET method. Palladium dispersion was determined by pulsed CO chemisorption at 35 °C using an Ar flow of $20\ ml\ min^{-1}$ and pulses of 0.2 ml of 10% CO in Ar. Prior to CO uptake determination all samples were treated under flowing hydrogen ($50\ ml\ min^{-1}$) and then flushed by Ar ($20\ ml\ min^{-1}$) for 60 min. In order to calculate the metal dispersion, an adsorption stoichiometry of $Pd/CO = 1$ was assumed [25].

Catalyst structures were characterised by powder X-ray diffraction using an Enraf Nonius PSD120 diffractometer with a monochromatic $CuK\alpha_1$ source operated at 40 keV and 30 mA. Experimental patterns were calibrated against silicon standard and phases were identified by matching experimental patterns to the JCPDS powder diffraction file.

Raman spectra were recorded using a Renishaw system 1000 dispersive laser Raman microscope. An argon ion laser (514.5 nm) was used as the excitation source and was typically operated at a power of 20 mW. Samples were used in powdered form and were placed on a microscope slide and the laser was focused onto the sample to produce a spot size of ca. 3 μm in diameter. Spectra were collected using a backscattering geometry with a 180° angle between the illuminating and the collected radiation.

Temperature-programmed reduction (TPR) was carried out in a Micromeritics Autochem 2910 equipped with a TCD detector. The reducing gas used in all experiments was 10% $H_2$ in Ar, with a flow rate of $50\ ml\ min^{-1}$. The temperature range explored was from room temperature to 650 °C. The heating rate was maintained at $10\ ^\circ C\ min^{-1}$ for all samples while the sample mass was varied depending on the sample under study. Details of specific conditions are given with the TPR profiles.

Table 1
Chemical composition, BET surface area, TPR hydrogen consumption, vanadium coverage, number of Pd sites, and Pd dispersion of the catalysts

| Catalysts | Pd (%) | V (%) | $S_{BET}$ | $H_2$ consumption (μmol-$H_2/g_{cat}$)[a] | $\theta$[b] | Pd sites/$g_{cat}$ ($\times 10^{-16}$)[c] | Pd dispersion[c] (%) |
|---|---|---|---|---|---|---|---|
| 0.5PdT | 0.5 | 0.0 | 50 | −1 | 0 | 52 | 34 |
| 0.5Pd0.5VT | 0.5 | 0.5 | 47 | 31 | 24 | 32 | 21 |
| 0.5Pd1.0VT | 0.5 | 1.0 | 47 | 45 | 48 | 22 | 14 |
| 0.5Pd1.5VT | 0.5 | 1.5 | 45 | 313 | 73 | 20 | 13 |
| 0.5Pd3.0VT | 0.5 | 3.0 | 39 | 563 | 147 | 14 | 9.0 |
| 1.0Pd1.5VT | 1.0 | 1.5 | 39 | 138 | 73 | 14 | 9.3 |
| 2.0Pd1.5VT | 2.0 | 1.5 | 40 | 116 | 73 | 2.8 | 1.8 |

[a] Data obtained by TPR.
[b] Fraction of vanadium monolayer (%), assuming a surface coverage of 0.2 $nm^2$ per $VO_x$ species [24].
[c] Data obtained by CO chemisorption.

Electron paramagnetic resonance measurements were performed using ca. 5 mg of catalyst, which was placed into a high-purity quartz EPR cell, fitted with an appropriate adaptor for connection to a vacuum manifold. The samples were evacuated to a residual pressure of $10^{-5}$ mbar before measurement, in order to remove air from the cell. The EPR spectra were recorded on a CW X-band Bruker EMX series spectrometer operating at 100 kHz field modulation in a Bruker ER4102ST standard cavity. All EPR spectra were recorded at 298 or 120 K. Accurate $g$ values were obtained using a Bruker ER 035 M NMR Gaussmeter.

### 2.3. Catalytic activity

Catalyst activity was determined using a fixed-bed laboratory microreactor. Catalysts were tested in powdered form using a $\frac{1}{4}$-inch o.d. stainless-steel reactor tube. The reaction feed consisted of 5000 vppm hydrocarbon in air. A total flow rate of 50 ml $min^{-1}$ was used and catalysts were packed to a constant volume to give a gas hourly space velocity of 40,000 $h^{-1}$ for all studies. Analysis was performed by an on-line gas chromatograph with thermal conductivity and flame ionisation detectors. Catalytic activity was measured over the range 100–550 °C and temperatures were measured by a thermocouple placed in the catalyst bed. Conversion data were calculated by the difference between inlet and outlet concentrations and all carbon balances were in the range $100 \pm 10\%$. Blank runs showed no conversion in the temperature interval studied for each alkane.

## 3. Results

### 3.1. Catalyst characterisation

Table 1 shows the BET surface areas, theoretical vanadium monolayer coverage, number of Pd sites, and the Pd dispersion for the catalysts synthesised in this study. As expected there was a reduction of the catalyst surface area as Pd and/or V loading increased. In addition, a dramatic decrease of the number of Pd sites, determined by CO chemisorption, was observed when the V and/or Pd loadings were increased. The catalyst without vanadium had a dispersion of palladium higher than 30%. However, the addition of vanadium content of 3 wt% decreased the Pd dispersion to less than 10%. Moreover, the increase of the Pd content also resulted in a drastic decrease in the number of available Pd sites. In fact, 2.0Pd1.5VT only had a dispersion of 2%. In Table 1, the monolayer coverage was estimated taking into account that each $VO_x$ unit occupies 0.2 $nm^2$ [24]. As can be observed in Table 1, the theoretical vanadium coverage of the catalysts ranged from 25 to 150%.

Raman spectra of the catalysts recorded in the 800–1100 $cm^{-1}$ range are shown in Figs. 1 and 2. Depending on the catalyst composition, three main vanadium bands centred at 920, 997, and 1028 $cm^{-1}$ were observed. The first absorption band centred at 920 $cm^{-1}$ is a broad band from 900 to 950 $cm^{-1}$, and it has been attributed to the terminal V=O stretching vibration of polyvanadate groups [26–29]. A second band, narrower than the first, and centred at 997 $cm^{-1}$ has been assigned to the presence of crystalline $V_2O_5$ [27–30]. Finally, at 1028 $cm^{-1}$ an absorption band characteristic of isolated tetracoordinated vanadium species bond with the support surface was observed [26–29].

Catalysts with varying vanadium contents without palladium were prepared for comparative purposes. Fig. 1 shows the Raman spectra for $V/TiO_2$ catalysts and 0.5% $Pd/V/TiO_2$ catalysts with different vanadium loadings. The $V/TiO_2$ catalyst with 1.5 wt% vanadium showed low-intensity bands at 997 and 920 $cm^{-1}$ corresponding to isolated and polymeric vanadium species. However, the catalyst with the same vanadium loading but with palladium showed the band at 920 $cm^{-1}$ with a much greater intensity. The Raman band corresponding to $V_2O_5$ crystallites was not detected in these catalysts. For samples with a 3 wt% vanadium the three bands associated with the different vanadium species were present in both V and Pd/Vcatalysts. However, the intensity of all species was higher in the palladium-containing catalyst. In general, the formation of polymeric species was favoured by the presence of palladium, since the band at 920 $cm^{-1}$ was more intense in $Pd/V/TiO_2$ catalysts than in $V/TiO_2$.

The evolution of vanadium species when the palladium content was increased was also probed by Raman spec-

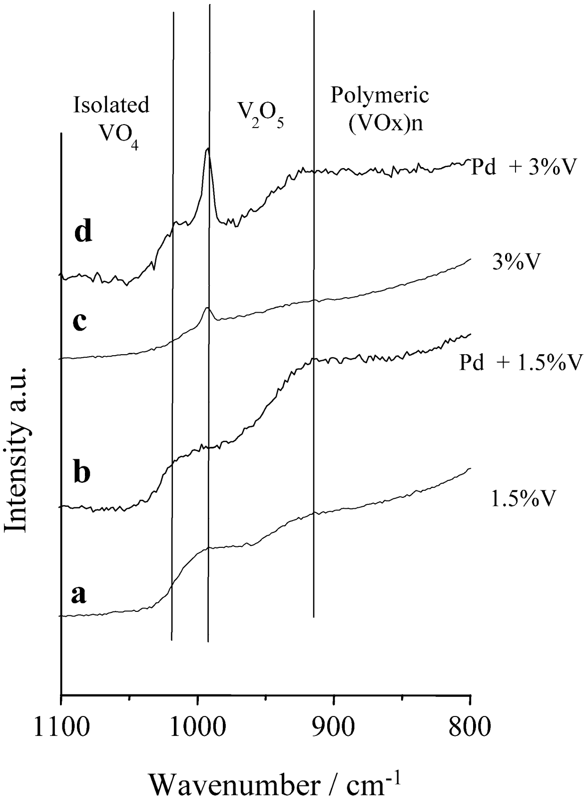

Fig. 1. Raman spectra of unpromoted and Pd-promoted vanadia titania catalysts from 800 to 1100 $cm^{-1}$ with varying vanadium loadings. (a) 1.5% $V/TiO_2$; (b) 0.5% Pd/1.5% $V/TiO_2$; (c) 3% $V/TiO_2$; and (d) 0.5% Pd/3.0% $V/TiO_2$.

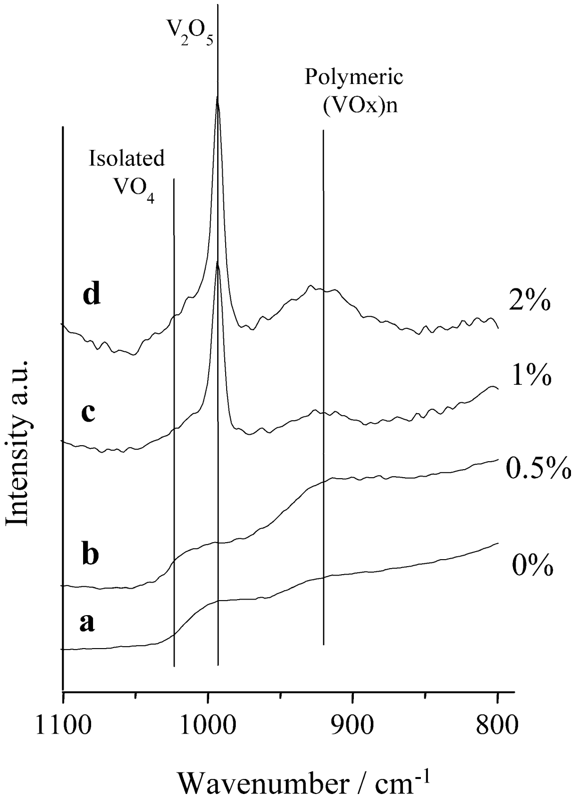

Fig. 2. Raman spectra of unpromoted and Pd-promoted vanadia titania catalysts with varying palladium loadings. (a) 1.5% $V/TiO_2$; (b) 0.5% Pd/1.5% $V/TiO_2$; (c) 1.0% Pd/1.5% $V/TiO_2$; and (d) 2.0% Pd/1.5% $V/TiO_2$.

troscopy (Fig. 2). The catalyst without palladium showed mainly isolated $VO_4$ species. The addition of 0.5 wt% Pd increased the intensity of the band corresponding to polymeric V–O–V species. Higher Pd content led to the observation of the characteristic band of $V_2O_5$. Therefore, the presence of palladium tended to increase the coordination and/or aggregation of vanadium species.

Raman spectroscopy was also used to investigate the influence of palladium and vanadium on the $TiO_2$ support. The region showing the main Raman bands of $TiO_2$ and the comparison of representative catalysts is shown in Fig. 3. The addition of vanadium to the titania produced a shift of the $TiO_2$ Raman active vibrations to a lower frequency. These observations clearly indicate that the support was modified by impregnation with vanadium. No further shifts were observed when palladium was added.

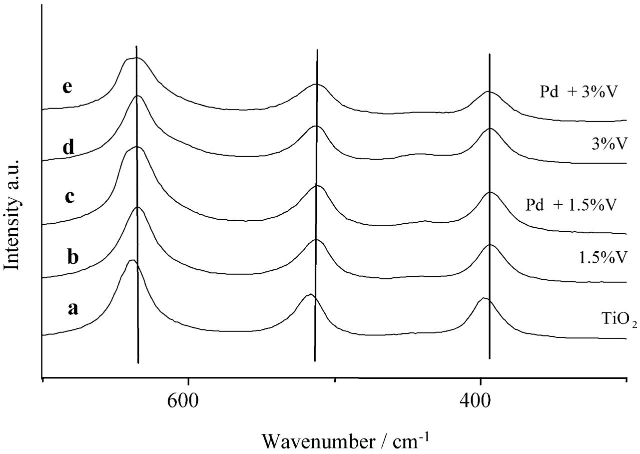

Fig. 3. Raman spectra of titania based catalysts from 300 to 700 $cm^{-1}$. (a) $TiO_2$; (b)1.5% $V/TiO_2$; (c) 0.5% Pd/1.5% $V/TiO_2$; (d) 3% $V/TiO_2$; and (e) 0.5% Pd/3.0% $V/TiO_2$.

Temperature-programmed reduction assays are shown in Figs. 4 and 5. TPR profiles demonstrated distinct differences between $V/TiO_2$ and $Pd/V/TiO_2$ catalysts. The $V/TiO_2$ catalysts (Fig. 4A) showed reduction peak maxima at temperatures between 350 and 425 °C. Three different maxima at 350–360, 390, and 420–430 °C were observed. These peaks were most likely related to three different vanadium species [30–34]. The catalysts with low V loading mainly showed the peak at 350 °C that can be related to the presence of isolated low-coordinated vanadium species. The presence of peaks at 390 and 425 °C increased with the vanadium loading, indicating the presence of polymeric $VO_x$ species and $V_2O_5$ crystallites, respectively.

TPR profiles of $Pd/V/TiO_2$ catalysts are reported in Fig. 4B. TPR data showed two or/three poorly defined reduction peaks between 50 and 125 °C, in contrast to the maxima at 350–425 °C observed for Pd-free catalyst reduction peaks. The assignment of these peaks is not clear but

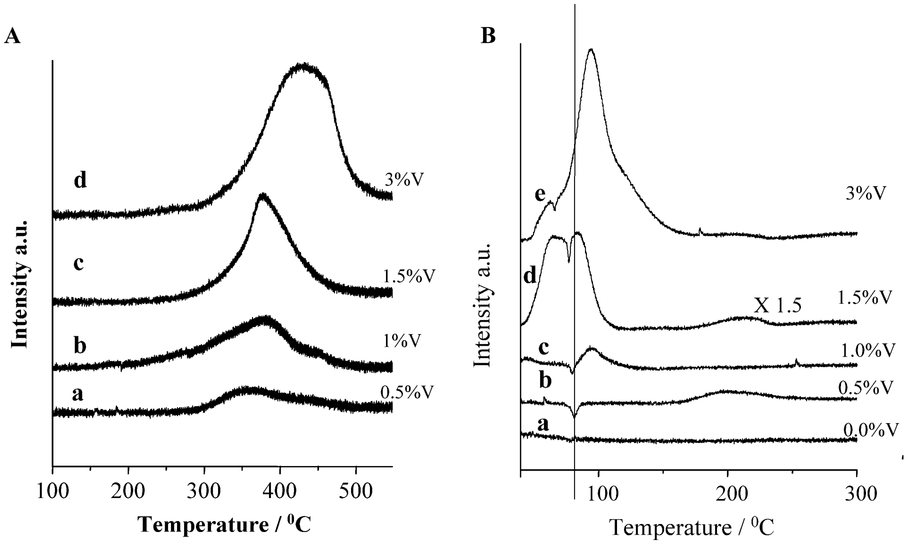

Fig. 4. TPR profiles of vanadium (A) and palladium-promoted vanadium (B) catalysts with varying vanadium loadings. (A) (a) 0.5% $V/TiO_2$; (b) 1.0% $V/TiO_2$; (c) 1.5% $V/TiO_2$; and (d) 3.0% $V/TiO_2$. (B) (a) 0.5% $Pd/TiO_2$; (b) 0.5% Pd/0.5% $V/TiO_2$; (c) 0.5% Pd/1.0% $V/TiO_2$; (d) 0.5% Pd/1.5% $V/TiO_2$; and (e) 0.5% Pd/3.0% $V/TiO_2$.

they may be related to partial reduction of $VO_x$ species in close contact with the palladium [24] and/or to the presence of highly dispersed palladium oxide [19]. Experimental results (Table 1) showed that the hydrogen consumption for the low-temperature reduction peak in 0.5% Pd/1.5% $V/TiO_2$ and 0.5% Pd/3.0% $V/TiO_2$ was 313 and 563 μmol-$H_2$ $g_{cat}^{-1}$, respectively. These values were considerably greater than the amount of hydrogen corresponding to the complete reduction of palladium oxide (47 μmol-$H_2$ $g_{cat}^{-1}$). Furthermore, hydrogen consumption at high temperatures, as observed for the $V/TiO_2$ catalysts, was not detected. These results suggest that vanadium oxide reduction also occurred in the temperature range 50–150 °C. Therefore, it can be concluded that the reducibility of vanadium sites was dramatically enhanced for $Pd/V/TiO_2$ catalysts when compared to $V/TiO_2$.

TPR profile of V-free Pd-catalyst is reported in Fig. 4B. TPR data showed a small negative peak at ca. 80 °C. The peak at 80 °C has been related to the release of hydrogen from the decomposition of palladium hydride species [35]. TPR assays have been carried out from 30 °C and usually the main reduction peaks of palladium, corresponding to $1.5H_2 + Pd^sO \rightarrow Pd^sH + H_2O$ and $(1 + \frac{1}{2}x)H_2 + Pd^bO \rightarrow Pd^bH_x + H_2O$ transitions [36], occur at subambient temperatures and therefore have not been recorded. It was also apparent that the reduction of palladium around 80 °C was more intense in the $Pd/V/TiO_2$ catalysts than in the 0.5% $Pd/TiO_2$ catalyst. It is known that the intensity of this peak is lower in samples with a high dispersion of palladium on the support surface [24]. This is in agreement with the data from Table 2 since the palladium dispersion of the 0.5% $Pd/TiO_2$ catalyst was considerably higher than that of the $Pd/V/TiO_2$ catalysts. It was also observed that the temperature at which the hydride decomposition peak occurred decreased when V loading increased.

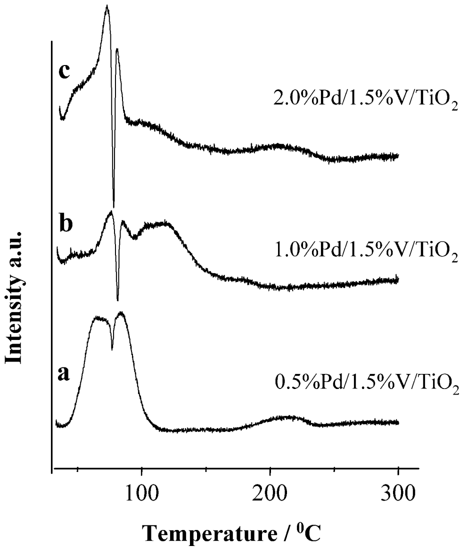

Fig. 5. TPR profiles of palladium-promoted vanadia titania catalysts with 1.5 wt% vanadium and different palladium loadings. (a) 0.5% Pd/1.5% $V/TiO_2$; (b) 1.0% Pd/1.5% $V/TiO_2$; and (c) 2.0% Pd/1.5% $V/TiO_2$.

Fig. 5 shows the TPR profiles for the catalysts with 1.5 wt% V and different Pd contents. Hydrogen consumption peaks between 50 and 90 °C were observed in 0.5% Pd/1.5% $V/TiO_2$ catalysts, while in 1.0% Pd/1.5% $V/TiO_2$ a 2.0% Pd/1.5% $V/TiO_2$ a shift to higher temperatures (up to 125 °C) was recorded. The shift was particularly prominent for the catalyst with 1 wt% of Pd. The negative palladium peak ca. 80 °C was present in all the samples; furthermore, as the Pd content was increased the area of the peak also increased. Thus, 2.0% Pd/1.5% $V/TiO_2$ catalyst showed a very intense signal due to both its very low dispersion of palladium (2%) and a high Pd content.

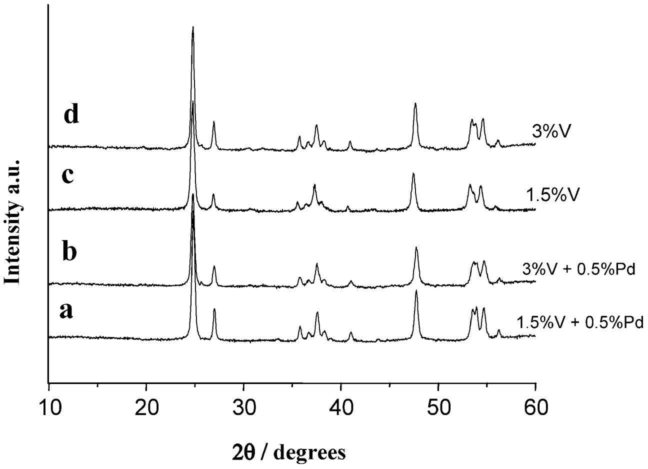

Fig. 6. Powder X-ray diffraction patterns: (a) 0.5% Pd/1.5% V/TiO$_2$; (b) 0.5% Pd/3.0% V/TiO$_2$; (c) 1.5% V/TiO$_2$; and (d) 3.0% V/TiO$_2$.

Powder XRD patterns of V/TiO$_2$ and Pd/V/TiO$_2$ catalysts do not provide significant additional information (Fig. 6). Diffraction peaks corresponding to TiO$_2$ anatase, and in minor quantity TiO$_2$ rutile, were detected in all the catalysts. No catalyst showed peaks corresponding to V-containing crystalline phases or metallic Pd. The presence of PdO cannot be ruled out in the catalysts with palladium.

The room temperature X-band EPR spectra for the 1.5% and 3% V/TiO$_2$ samples are shown in Fig. 7. The corresponding spectra for the 1.5 and 3% V/TiO$_2$ catalysts promoted with 0.5% Pd are shown in Fig. 8. The EPR spectra can be readily assigned to the d$^1$ vanadium ion (width $I = 7/2$), producing the characteristic 8 line hyperfine spectrum [37]. No underlying signals associated with paramagnetic centres originating from the TiO$_2$ support [38,39], or indeed any paramagnetic palladium species [40], were detected. The spin Hamiltonian parameters were determined by computer simulation using the Bruker SIMFONIA software, which revealed a slightly rhombic $g$ and $A$ tensors ($g_1 = 1.970 \approx g_2 = 1.965$ or $g_\perp$ and $g_3 = 1.938$ or $g_\perp$; $A_1 = 58$ G $\approx A_2 = 56$ G or $A_\perp$ and $A_3 = 178$ G or $A_{||}$). While the resolution and intensity of the spectra changed markedly for each sample, this set of spin Hamiltonian parameters remained very similar (within the resolution of the spectra). These parameters are typical of those expected for surface-supported V$_2$O$_5$ oxide [41–43], and clearly evidence the presence of paramagnetic vanadium oxide species in these freshly prepared catalysts.

### 3.2. Alkane oxidation activity

The main reaction product observed during the propane oxidation over Pd/TiO$_2$ and Pd/V/TiO$_2$ catalysts was CO$_2$, with selectivities always greater than 99.5%. Traces of methane, CO, and propene were also detected in a minority of experiments. For the V/TiO$_2$ catalysts higher selectivities to the olefin were observed, although they never exceeded 1%. It has been reported that vanadium supported on titanium oxide can oxidatively dehydrogenate propane to propylene with moderate selectivities [44]. However, the high oxygen concentration (O$_2$/alkane ratio of 40) employed in the present work favours the deep oxidation of the olefin, preventing its formation with high selectivities.

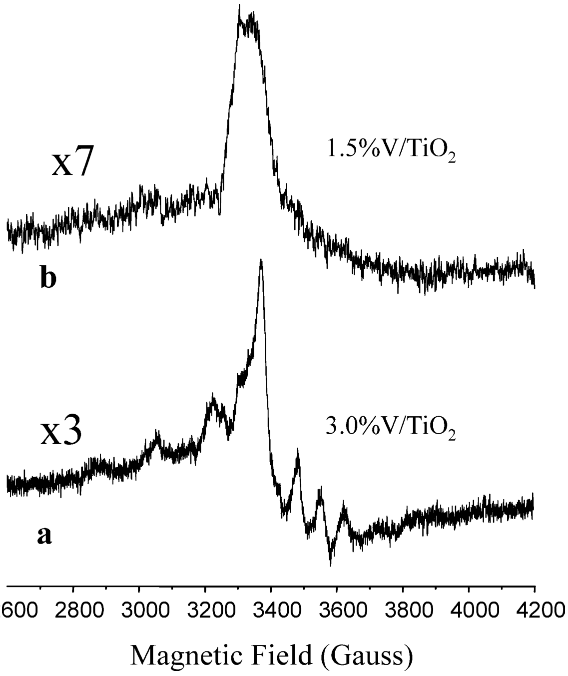

Fig. 7. EPR spectra of V/TiO$_2$ catalysts with different vanadium loadings. (a) 3.0% V/TiO$_2$ and (b) 1.5% V/TiO$_2$.

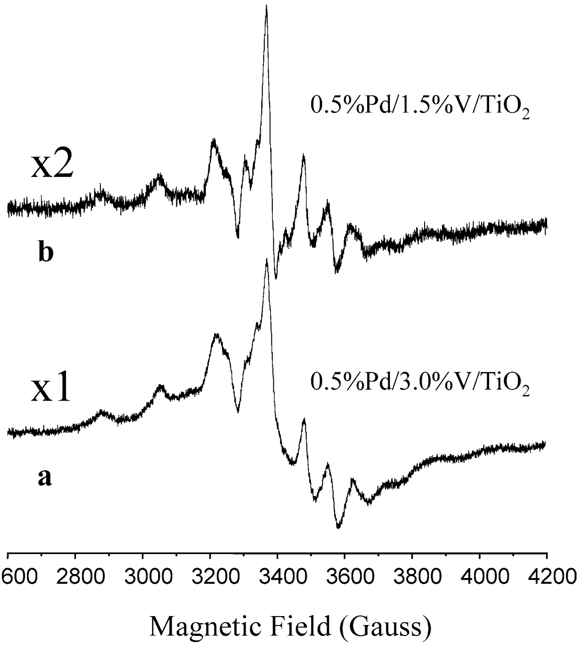

Fig. 8. EPR spectra of Pd-promoted catalysts with different vanadium loadings. (a) 0.5% Pd/3.0% V/TiO$_2$ and (b) 0.5% Pd/1.5% V/TiO$_2$.

Fig. 9 compares the catalytic activity for propane oxidation by catalysts with 0.5 wt% Pd and different vanadium loadings. Different catalytic behaviour was observed

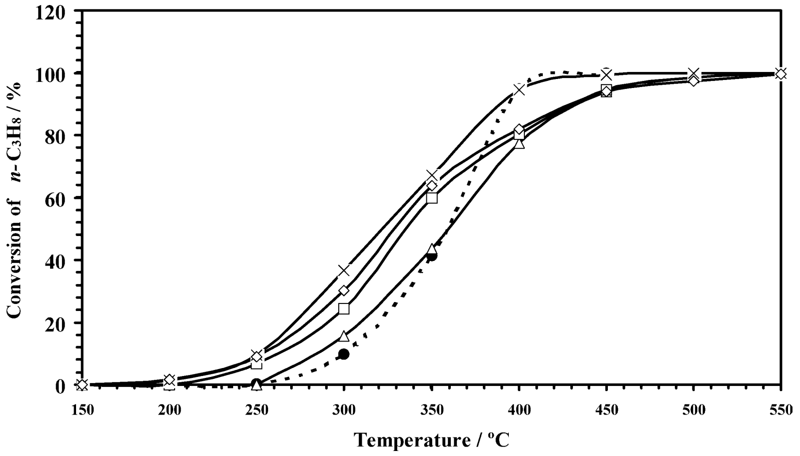

Fig. 9. Propane conversion over Pd-promoted V/$TiO_2$ catalysts with varying vanadium loadings as a function of reaction temperature. ●, 0.5% Pd/$TiO_2$; △, 0.5% Pd/0.5% V/$TiO_2$; □, 0.5% Pd/1.0% V/$TiO_2$; ×, 0.5% Pd/1.5% V/$TiO_2$; and ◇, 0.5% Pd/3.0% V/$TiO_2$.

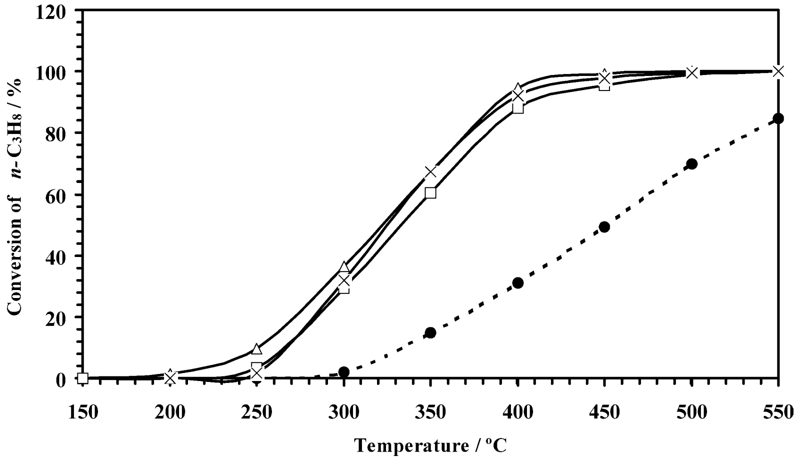

Fig. 10. Propane conversion over Pd-promoted V/$TiO_2$ catalysts with varying palladium loadings as a function of reaction temperature. ●, 1.5% V/$TiO_2$; △, 0.5% Pd/1.5% V/$TiO_2$; □, 1.0% Pd/1.5% V/$TiO_2$; and ×, 2.0% Pd/1.5% V/$TiO_2$.

between the Pd/$TiO_2$ catalyst and the Pd/V/$TiO_2$ catalysts, since the addition of vanadium to Pd/$TiO_2$ significantly decreased the light-off temperature of propane. At the lower reaction temperatures of 250 and 300 °C Pd/V catalysts showed much higher propane conversion than the catalyst with Pd alone. It was clearly observed that the presence of vanadium in the Pd/$TiO_2$ catalyst greatly increased the catalytic combustion at low temperatures and the activity of the Pd/V/$TiO_2$ was dependent on the amount of vanadium present. The optimal vanadium content corresponded to 1.5 wt%, which was equivalent to a surface coverage of $VO_x$ species of 75% of a theoretical monolayer. A further increase in the vanadium loading led to a decrease in the catalytic activity.

Fig. 10 shows the evolution of the propane conversion with reaction temperature for catalysts with a 1.5 wt% V and different palladium contents. The Pd-free catalyst showed low activity, demonstrating initial activation of propane at 350 °C. However, the addition of Pd increased the catalytic activity of the Pd/V/$TiO_2$ catalysts. For example, the light off and $T_{50}$ (temperature for 50% propane conversion) for Pd-containing catalysts were 250–300 and 325 °C, respectively, whereas for the vanadium catalyst were 350 and 450 °C. Surprisingly, the propane conversion obtained over 0.5% Pd/1.5% V/$TiO_2$, 1.0% Pd/1.5% V/$TiO_2$ and 2.0% Pd/1.5% V/$TiO_2$ were essentially independent of the concentration of palladium present (Fig. 10), although it may be expected that the increased Pd content would be accompanied by an increase of catalytic activity. The decrease in the dispersion of palladium when Pd-loading increased and the active role of vanadium sites could explain the behaviour observed.

The catalyst stability of 0.5% Pd/$TiO_2$ and 0.5% Pd/1.5% V/$TiO_2$ was studied at various reaction temperatures. No deactivation was observed in any of the samples after 76 h time on line. These results can be observed in Fig. 11, where the propane conversions in terms of the time on stream for 0.5% Pd/$TiO_2$ and 0.5% Pd/1.5% V/$TiO_2$ catalysts at 300 and 325 °C are shown.

Table 2 shows the propane conversion obtained by some representative Pd and Pd/V catalysts at 250 and 300 °C. For comparison a commercial Pd/alumina catalyst (PdA COMM, 5 wt% Pd, $S_{BET} = 140\ m^2\,g^{-1}$) is included in the

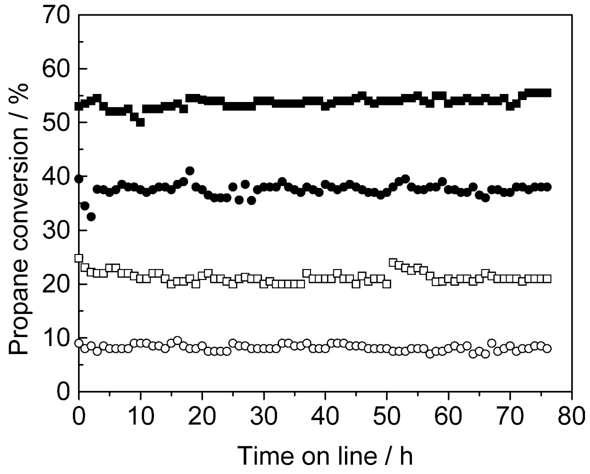

Fig. 11. Propane conversion over 0.5% $Pd/TiO_2$ and 0.5% Pd/1.5% $V/TiO_2$ catalysts at different temperatures as a function of time on stream: 300 °C, ●, 0.5% Pd/1.5% $V/TiO_2$; ○, 0.5% $Pd/TiO_2$. 325 °C, ■, 0.5% Pd/1.5% $V/TiO_2$; □, 0.5% $Pd/TiO_2$.

Table 2
Propane conversion at low reaction temperatures of Pd catalysts and palladium-promoted vanadium catalysts

| Catalyst | Reaction temperature (°C) | |
|---|---|---|
| | 250 | 300 |
| PdA COMM | 0 | 16 |
| 0.5PdT | 0 | 9 |
| 0.5Pd1.5VT | 10 | 37 |
| 2.0Pd1.5VT | 2 | 32 |

table. At 250 °C no Pd-supported catalyst showed activity whereas V/Pd catalysts activate the alkane. In addition, at 300 °C the propane conversions for Pd catalysts were around 10% while for V/Pd catalysts conversions were in the region of 40%. It must be noted that a V/Pd catalyst with only 0.5 wt% Pd can activate the propane at 50 °C lower than the $Pd/Al_2O_3$ catalyst with a Pd content 10 times higher.

In order to probe whether the addition of vanadium to $Pd/TiO_2$ catalysts improved the catalytic performance for other short-chain alkanes, activity studies for methane, ethane, and *n*-butane were performed. Comparison was made with the 5% $Pd/Al_2O_3$ catalyst. Table 3 shows the alkane conversions obtained at different temperatures. It is recognised that the alkanes are more difficult to oxidise to $CO_2$ as the carbon number decreases. This trend is reflected by the data, as there was a successive increase in light-off temperature from *n*-butane to methane. Both catalysts produced $CO_2$ as the only oxidation product. The 0.5% Pd/1.5% $V/TiO_2$ catalyst had a lower light-off temperature for *n*-butane, propane, ethane, and methane when compared to the 5% $Pd/Al_2O_3$ catalyst. Moreover, appreciable rates of hydrocarbon oxidation were observed for the alkanes over 0.5% Pd/1.5% $V/TiO_2$ at temperatures where the 5% $Pd/Al_2O_3$ catalyst was inactive. The rate of methane oxidation was greater over 5% $Pd/Al_2O_3$ than 0.5% Pd/1.5% $V/TiO_2$ above 350 °C.

## 4. Discussion

Studies on the modification of Pd-based catalysts by addition of different promoting agents, usually metals or metal oxides, for short-chain alkane oxidation, especially methane, are extensive [20–24]. However, studies on modified $Pd/TiO_2$-based catalysts are limited. This work shows that the addition of vanadium to Pd-based $TiO_2$ catalysts decreased the light-off temperature during the total oxidation of short-chain alkanes and significantly increases the rates of oxidation at lower temperatures. This work has focused on catalyst characterisation in order to probe the important characteristics for the enhanced activity. Several crucial questions concerning the supported vanadium catalysts are in active discussion in the literature—the role of the support, the vanadium loading, the strength of V=O bond, the reducibility of the V–O-support bond, and the nature of the active vanadium species [41]. Characterisation of the catalysts in this study has helped to define the role of these parameters.

Raman spectroscopy was used to study the nature of the vanadium species. It followed from the analysis of the Raman data (Fig. 1) that polyvanadate species were predominantly observed in the nonpromoted and Pd-promoted $V/TiO_2$ samples at high vanadium loading, and only a small amount of monovanadate species coexisted on the surface of the titania support. The Raman spectra of 0.5% Pd/3% $V/TiO_2$ showed that $V_2O_5$ crystallites were only present at vanadium coverages higher than the monolayer. On the other hand, it was observed that an increase of the palladium content in 1.5% $V/TiO_2$ catalysts ranging from 0 to 2% produced an increase in the aggregation and/or coordination of vanadium species (Fig. 2). In these catalysts, $V_2O_5$ crystallites were detected at Pd loadings of 1% and higher. Therefore, it can be concluded that the addition of palladium increased the amount of polyvanadate species and $V_2O_5$ crystallites on the surface of $Pd/V/TiO_2$ catalysts, but no major modification of the nature of the vanadium species was detected, as the same Raman bands were present although with differing relative intensities.

It is interesting to note that, from Raman data, modification of the support in both $V/TiO_2$ and $Pd/V/TiO_2$ catalysts was observed, and it appeared this was mainly due to vanadium. The shift of frequency of the $TiO_2$ vibrations indicates that there is interaction between the supported vanadium species and the $TiO_2$. By the nature of the reflected radiation Raman spectroscopy is more sensitive to the catalyst surface. Conversely X-ray diffraction is a bulk characterisation technique and studies showed that there was no discernable structural modification of the $TiO_2$ support when vanadium was added.

In relation to the Raman conclusions, it is worth noting that a new assignment of vanadium Raman bands has recently been reported [45]. Interestingly it is claimed that in general the vanadyl vibrations cannot be assumed to be independent of the substrate and thus cannot be used as an indi-

Table 3
Comparison of the conversion of short-chain alkanes over $Pd/Al_2O_3$ and 0.5% Pd/1.5% $V/TiO_2$ catalysts

| Alkane | Catalyst | Reaction temperature (°C) | | | | | | | |
|---|---|---|---|---|---|---|---|---|---|
| | | 200 | 250 | 300 | 350 | 400 | 450 | 500 | 550 |
| Methane | 1.5VPdT | 0.0 | 1.0 | 3.2 | 7.3 | 15 | 31 | 56 | 75 |
| | PdA COMM | 0.0 | 0.0 | 1.0 | 7.3 | 54 | 94 | 100 | 100 |
| Ethane | 1.5VPdT | 0.0 | 4.0 | 16 | 35 | 71 | 99 | 100 | 100 |
| | PdA COMM | 0.0 | 0.0 | 11 | 44 | 88 | 100 | 100 | 100 |
| Propane | 1.5VPdT | 0.0 | 9.6 | 37 | 67 | 95 | 99 | 100 | 100 |
| | PdA COMM | 0.0 | 0.0 | 16 | 50 | 90 | 100 | 100 | 100 |
| *n*-Butane | 1.5VPdT | 0 | 11.7 | 43 | 75 | 95 | 100 | 100 | 100 |
| | PdA COMM | 0 | 0 | 21 | 95 | 99 | 100 | 100 | 100 |

cator for monomeric and polymeric species. Unfortunately, this work was carried out with silica and alumina supports and there is no available data for other supports such as $TiO_2$. Therefore, these new Raman interpretations may make the specific assignment of titania-supported vanadium bands more difficult. However, the overall general conclusions are not altered as the data in this study still show that the vanadium species are modified by varying the vanadium loading and by the addition of palladium.

TPR studies were used to evaluate the reducibility of the vanadium species. It has been observed that the incorporation of palladium to $V/TiO_2$ catalysts led to a dramatic increase in the reducibility of vanadium. Moreover, the increase of the vanadium loading in $Pd/V/TiO_2$ catalysts led to a decrease in the reducibility of vanadium. This behavior was also seen for the nonpromoted $V/TiO_2$ samples.

As postulated by Bond and Tahir [46], upon increasing the $V_2O_5$ loading on titania, layers of "*disordered*" $V_2O_5$ and "*paracrystalline*" $V_2O_5$ phases are formed on limited areas of the surface. These $V_2O_5$ crystallites are more difficult to reduce than coordinated species, and therefore, a peak at higher temperatures due to the reduction of these species is registered (Fig. 4). By analogy with nonpromoted catalysts, we assigned the very broad band for the 0.5% Pd/3% $V/TiO_2$ sample to the presence of $V_2O_5$ crystallites along with the $VO_x$ monolayer species. Raman spectra of these samples also gave evidence for small particles of $V_2O_5$ at high vanadium loading.

Several groups have previously observed that the addition of palladium strongly promoted the reduction of vanadium oxide at lower temperatures on alumina-supported catalysts. Dancheva et al. [47] studied 30% $V_2O_5/Al_2O_3$ and Pd/30% $V_2O_5/Al_2O_3$ catalysts by TPR. The TPR profile of 30% $V_2O_5/Al_2O_3$ exhibited a peak at 530 °C, whereas the Pd/30% $V_2O_5/Al_2O_3$ catalyst showed reduction at a lower temperature (140 °C). In the same way, Ferreira et al. [48] studied different $V_2O_5$ loadings on $Pd/Al_2O_3$ ranging from 5 to 20%. These authors also observed a strong promoting effect of palladium on the vanadium oxide reduction. According to these authors, hydrogen is activated on metallic palladium through dissociative adsorption to atomic hydrogen, which promoted the reduction of vanadium oxide. This interpretation was also given by other authors to explain the promoting effect of other metal oxides on $Pd/Al_2O_3$ catalysts; these oxides include $Nb_2O_5$ [49], $CeO_2$ [50], and $MoO_3$ [51]. An alternative explanation of the reduction behaviour was proposed by Neyertz and Volpe [24], who suggested that the reduction of $VO_x$ species takes place at the expense of a fraction of Pd that remains in an oxidised state. Moreover, Neyertz and Volpe also suggested that a fraction of oxidized palladium that cannot be reduced at low temperature could be reduced along with the $VO_x$ species.

We consider that the increased ease of vanadium reduction on the titania support by the addition of palladium operates by a spillover mechanism that has been identified on similar alumina-supported catalysts [47,48]. In such a mechanism hydrogen dissociatively chemisorbed at the palladium surface and the resulting atomic hydrogen species effect vanadium reduction. The reduction of vanadium can proceed via formation of a vanadium bronze, and it has been demonstrated that such a phase can be formed on alumina-supported catalysts at temperatures as low as 100 °C [52].

The EPR data was used to estimate the influence of the support and of palladium on the vanadyl bond strength. It is possible to discriminate between the nature and the symmetry of the supported vanadium ions by careful analysis of the low-temperature EPR spectra, as demonstrated by Dyrek et al. [44]. By calculating the crystal field parameters ($\Delta$ and $\delta$) from the EPR spectra using the equations $g_{||} = g_e(1-4l/\Delta)$ and $g_\perp = g_e(1 - l/\delta)$ (suitable for $V^{4+}$ in distorted octahedral symmetry) information on the local environment surrounding the paramagnetic ion can be obtained since the parameter $D$ depends only on the V–O distance in the equatorial plane of the $VO_6$ octahedral, whereas d is a function of all V–O distances [42]. The crystal field parameters calculated from the spin Hamiltonian parameters in our samples are typical of those characteristics of hexacoordinated $V^{4+}$ ions in a highly distorted octahedron in the $V_2O_5$ lattice. However, these parameters were similar in the presence and absence of palladium (i.e., Fig. 8 compared to Fig. 7). The only differences observed in the EPR spectra correspond to the relative intensities of the spectra. The EPR spectra for the vanadium-doped samples (both 1.5 and 3% $V/TiO_2$ in Fig. 7) are systematically lower (around 3 times) than those observed from the palladium-doped samples (Fig. 8). This indicates that while the codoped Pd influences the overall abundance of paramagnetic $V^{4+}$ ions (i.e., affecting the oxidation state of the supported vanadium ions) it does not structurally perturb the nature of the supported vanadium oxide species themselves.

There remains controversy about the effect of the noble metal particle size on catalytic hydrocarbon combustion. While several authors [53–55] have not observed a correlation between the particle size and the activity, others have shown a strong dependence between the activity and the particle size. Yazawa et al. [55] suggest for propane combustion that although both the dispersion and the oxidation states of palladium affect the catalytic activity on a series of supports, the oxidation state of palladium affects the catalytic activity more than the dispersion. The partially oxidized palladium showed the highest catalytic activity for propane combustion. Thus, the addition of vanadium to Pd catalysts could prevent the total oxidation of palladium, as observed by Neyertz and Volpe [24], and therefore, increase the propane combustion activity. Again this suggestion could not be probed directly due to the limitations of the TPR technique. On the other hand, Hicks et al. [7] showed that highly dispersed palladium oxide could be very much less active than crystalline palladium oxide supported on alumina. The palladium with a small crystallite size exhibited lower activity due to the strong interaction with the support $Al_2O_3$. [7]. From the CO chemisorption data, it has been observed that the number of palladium sites decreases with the incorporation of vanadium. This decrease could be due to two different effects: (i) an increase of the palladium aggregation; (ii) the coverage of the palladium sites by the vanadium during the coimpregnation step. As it was shown above, TPR profiles gave a hydrogen release peak at $\sim 83\,^{\circ}C$ due to hydride decomposition. The intensity of this peak was independent of the vanadium concentration in the different catalysts. This is evidence of the coverage of the palladium sites, as has been suggested by Neyertz and Volpe [24]. On the other hand, the increase of the palladium content in Pd/1.5% $V/TiO_2$ catalysts produced a dramatic decrease in the palladium dispersion. This fact is most likely due to an increase of the palladium aggregation, because comparison between the TPR profiles of these samples, shown in Fig. 4, revealed considerably higher intensities for the hydrogen release peak when the palladium concentration increased. This increase in the amount of bulk palladium did not lead to an increase in the catalyst activity, and Yazawa et al. observed a similar effect on other supported palladium catalysts [55]. Indeed, similar or lower propane conversions were found when the palladium content was increased. Therefore, it can be suggested that the propane combustion on $Pd/V/TiO_2$ catalysts is not solely a palladium size-dependent reaction and the modification of the redox properties of the catalyst was also an important factor in determining catalyst activity.

In our opinion the main factor for the improvement of the catalytic behaviour of V/Pd-catalysts in comparison with unmodified Pd catalysts is the high reducibility of vanadium species. Thus, the promotional effect of vanadium can be related to the redox interchange and the effect of the palladium particles. In this way, the reducibility of vanadium species in the 0.5% Pd/3.0% $V/TiO_2$ catalyst is lower than in the 0.5% Pd/1.5% $V/TiO_2$ catalyst, and this was reflected in the lower activity of the catalyst with the higher vanadium loading (Fig. 8). In addition, the 1.0% Pd/1.5% $V/TiO_2$ catalyst, with lower vanadium reducibility due to the TPR peaks at higher temperatures (Fig. 5), showed lower catalytic activity in propane combustion (Fig. 9). There are data in the literature on the promotional effect of palladium over $Al_2O_3$-supported vanadium oxide for complete hydrocarbon oxidation. The effect has been related to the activation of oxygen on the metal particles, which enables the reverse oxidation of $V^{4+}$, and this leads to an equilibrium in the redox process [56]. These authors proposed a redox mechanism to explain the process: (i) oxidation of $V^{4+}$ to $V^{5+}$ and $Pd^0$ to $Pd^{2+}$ by the oxygen; (ii) reduction of $V^{5+}$ to $V^{4+}$ by the hydrocarbon. In this mechanism $V^{3+}$ was very stable. Our EPR and Raman results indicate that the presence of palladium does not structurally perturb the nature of vanadium or titanium species and a higher amount of $V^{4+}$ is present in V/Pd-catalysts, suggesting that the above redox mechanism could be operating.

## 5. Conclusions

It has been demonstrated that the activity of titania-supported palladium catalysts for the deep oxidation of short-chain alkanes is increased by modification with vanadium during the impregnation step of catalyst preparation. A vanadium loading of 1.5 with 0.5% palladium was the most active catalyst. The combination of vanadium and palladium modified the vanadium species on the catalyst, increased the concentration of $V^{4+}$, and increased the ease of catalyst reduction, which can help to explain the promotion of activity. At this stage little attempt has been made to optimise the activity of the $Pd/V/TiO_2$ catalyst. Against the background of this study these systems are now worthy of further investigation to establish their potential as environmental catalysts.

## Acknowledgment

T. Garcia thanks the Ministry of Education and Science, MEC, (Spain) for the FPU fellowship.

## References

[1] A.C. Lewis, N. Carslaw, P.J. Marriott, R.M. Kinghorn, P. Morrison, Lee, L. Andrew, K.D. Bartle, M.J. Pilling, Nature 405 (2000) 778.
[2] M.J. Molina, F.S. Rowland, Nature 249 (1974) 810.
[3] B.J. Finlayson-Pitts, J.N. Pitts, Science 276 (1997) 1045.
[4] EPA Publication No. EPA 454/R-03-005, Table a5, Environmental Protection Agency, Office of Air Quality and Standard, Air Quality

Strategies and Standards Division, Research Triangle Park, NC. This report can be found in http://www.epa.gov/air/aqtrnd03/toc.html.

[5] T.V. Choudhary, S. Banerjee, V.R. Choudhary, Appl. Catal. A 234 (2002) 1.

[6] R.B. Anderson, K.C. Stein, J.J. Feenan, L.J.E. Hofer, Ind. Eng. Chem. 53 (1961) 809.

[7] R.F. Hicks, H. Qi, M.L. Young, R.G. Lee, J. Catal. 122 (1990) 295.

[8] K. Narui, K. Furuta, H. Yata, Catal. Today 45 (1998) 173.

[9] R. Burch, F.J. Urbano, Appl. Catal. 124 (1995) 121.

[10] K. Eguchi, H. Arai, Appl. Catal. 222 (2001) 359.

[11] R.J. Farrauto, M.C. Hobson, T. Kennelly, E.M. Waterman, Appl. Catal. 81 (1992) 227.

[12] V. Labalme, E. Garbowski, N. Guilhaume, Appl. Catal. 138 (1996) 93.

[13] R. Spinicci, A. Tofanari, Appl. Catal. A 227 (2002) 159.

[14] K. Sekizawa, H. Widjaja, S. Maeda, Y. Ozawa, K. Eguchi, Catal. Today 59 (2000) 69.

[15] M.S. Waiwright, N.R. Foster, Catal. Rev. 19 (1979) 211.

[16] H. Bosch, F. Janssen, Catal. Today 2 (1988) 369.

[17] C.A. Müller, M. Maciejewski, R.A. Koeppel, A. Baiker, Catal. Today 47 (1999) 245.

[18] C.B. Wang, H.K. Lin, C.M. Ho, J. Mol. Catal. A: Chem. 180 (2002) 285.

[19] L.S. Escandón, S. Ordóñez, F.V. Diez, H. Sastre, Catal. Today 78 (2003) 191.

[20] H. Shaper, E.B.M. Doesburg, L.L. Van Reijen, Appl. Catal. 7 (1983) 211.

[21] M. Machida, K. Eguchi, H. Arai, J. Catal. 103 (1987) 385.

[22] G. Groppi, C. Cristiani, L. Lietti, C. Ramella, M. Valentini, P. Forzatti, Catal. Today 50 (1999) 399.

[23] P. Euzen, J.H. LeGal, B. Rebours, G. Martin, Catal. Today 47 (1999) 19.

[24] C. Neyertz, M. Volpe, Colloids Surf. A 136 (1998) 63.

[25] J.R. Anderson, Structure of Metallic Catalysts, Academic Press, London, 1975.

[26] I.E. Wachs, J. Catal. 124 (2) (1990) 570.

[27] I.E. Wachs, B.M. Weckhuysen, Appl. Catal. A 157 (1997) 67.

[28] G. Busca, L. Marchetti, G. Centi, F. Trifiro, Langmuir 2 (1986) 568.

[29] C.B. Rodella, R.W.A. Franco, C.J. Magon, J.P. Donoso, L.A.O. Nunes, M.J. Saeki, M.A. Aegerter, V. Sargentelli, A.O. Florentino, J. Sol Gel Sci. Technol. 83 (2002) 25.

[30] D.A. Bulushev, L. Kiwi-Minsker, F. Rainone, A. Renken, J. Catal. 115 (2002) 205.

[31] B. Solsona, T. Blasco, J.M. Lopez Nieto, M.L. Pena, F. Rey, A. Vidal-Moya, J. Catal. 203 (2001) 443.

[32] H. Berndt, A. Martin, A. Bruckner, E. Schreier, D. Muller, H. Kosslick, G.V. Wolf, B. Lucke, J. Catal. 191 (2000) 284.

[33] M. Baltes, K. Cassiers, P. Van der Voort, B.M. Weckhuysen, R.A. Schoonheydt, E.F. Vansant, J. Catal. 197 (2001) 160.

[34] J. Santamaria-Gonzalez, J. Luque-Zambrana, J. Merida-Robles, P. Maireles-Torres, E. Rodriguez-Castellon, A. Jimenez-Lopez, Catal. Lett. 68 (2000) 67.

[35] G. Chen, W.T. Chou, C.T. Yeh, Appl. Catal. 8 (1983) 389.

[36] G. Chen-Bin, L. Hung-Kuan, H. Chi-Man, J. Mol. Catal. A: Chem. 180 (2002) 285.

[37] D.M. Murphy, I.A. Fallis, R.D. Farley, R.J. Tucker, K.L. Avery, D.J. Willock, Phys. Chem. Chem. Phys. 4 (2002) 4937.

[38] C.A. Jenkins, D.M. Murphy, J. Phys. Chem. B 103 (1999) 1019.

[39] A. Attwood, J. Edwards, C.C. Rowlands, D.M. Murphy, J. Phys. Chem. B 107 (2003) 1779.

[40] L.S. Stokes, D.M. Murphy, R.D. Farley, C.C. Rowlands, S. Bailey, Phys. Chem. Chem. Phys. 1 (1999) 621.

[41] D. Andreeva, T. Tabakova, L. Ilieva, A. Naydenov, D. Mehanjiev, M.V. Abrashev, Appl. Catal. A 209 (2001) 291.

[42] J. Spengler, F. Anderle, E. Bosch, R.K. Grasselli, B. Pillep, P. Behrens, O.B. Lapina, A.A. Shubin, H.J. Eberle, H. Knozinger, J. Phys. Chem. B 105 (2001) 10772.

[43] K.V.R. Chary, T. Bhaskar, J.J. Maheshwar, K. Ramesh, V.V. Rao, Appl. Catal. A 202 (2000) 133.

[44] K. Dyrek, M. Labanowska, H. Rembertowicz, E. Bidzinska, Spectrochim. Acta A 56 (2000) 309.

[45] N. Magga, B. Immaraporna, J.B. Giorgi, T. Schroeder, M. Bäumer, J. Döbler, Z. Wu, E. Kondratenko, M. Cheriand, M. Baerns, P.C. Stair, J. Sauer, H.J. Freund, J. Catal. 226 (2004) 88–100.

[46] G.C. Bond, S.F. Tahir, Appl. Catal. A 71 (1991) 1.

[47] S. Dancheva, L. Ilieva, N. Kotsev, A. Andreev, Collect. Czech. Chem. Commun. 59 (1994) 1922.

[48] R.S.G. Ferreira , P.G.P. de Oliveira, F.B. Noronha, Appl. Catal. B 50 (2004) 243.

[49] F.B. Noronha, D.A.G. Aranda, A.P. Ordine, M. Schmal, Catal. Today 57 (2000) 169.

[50] R.S. Monteiro, F.B. Noronha, L.C. Dieguez, M. Schmal, Appl. Catal. A 131 (1995) 89.

[51] M. Schmal, M.A.S. Baldanza, M.A. Vannice, J. Catal. 185 (1999) 138.

[52] E. van der Heide, M. Zwinkels, A. Gemitsen, J. Sholten, Appl. Catal. A 86 (1999) 181.

[53] K. Muto, N. Katada, M. Niwa, Appl. Catal. 134 (1996) 203.

[54] T.R. Baldwin, R. Burch, Appl. Catal. 66 (1990) 337.

[55] Y. Yazawa, H. Yoshida, N. Takagi, S. Komai, A. Satsuma, T. Hattori, J. Catal. 187 (1999) 15.

[56] M. Vassileva, A. Andreev, S. Dancheva, N. Kotsev, Appl. Catal. 449 (1989) 125.